Article | Received 3 March 2026; Revised 28 July 2026; Accepted 1 September 2026; Published XX September 2026
https://doi.org/10.55092/aimat20260011

Data-efficient design of DOPO/rare-earth flame-retardant epoxy resins for carbon fiber composites

Peng Wang[1],*, Yunxuan Wang[1], Zheng Wang[1], Yingjie Qiao[2], Liangshuo Zhao[2], Lei Shi[3], Jiajie He[3], Shujing Yue[3] and Zhaoding Yao[3]

[1] School of Materials Science and Engineering, China University of Petroleum (East China), Qingdao, China
[2] Material Science and Chemical Engineering, Harbin Engineering University, Harbin, China
[3] CRRC Advanoed Composites Co., Ltd., Qingdao, China

* Correspondence author; E-mail: 20230026@upc.edu.cn.

Highlights:

- A "parameterization-visualization" dual-driven strategy overcomes data sparsity, enabling rapid identification of the optimal 48.3D/63.9R formulation with minimal trials.
- The optimized resin achieves superior flame retardancy via gas-phase/condensed-phase synergy, meeting stringent processing and mechanical requirements for large-tow composites.

Abstract: To address the challenges of data sparsity and model generalization in small-sample material optimization for flame-retardant resin matrices in composites, this study proposes a "parameterization-visualization" dual-driven strategy. This approach establishes an efficient, standardized pathway for AI-driven material development without relying on black-box algorithms. First, bivariate experimental data involving 10-(2,5-dihydroxyphenyl)-10H-9-oxa-10-phospha-phenanthrene-10-oxide (DOPO-HQ) and a self-developed R-powder (composed of Y_2O_3-stabilized borophosphate glass, zinc borate, and SiO_2) were utilized to generate a high-resolution performance matrix via contour interpolation, thereby transforming sparse experimental points into continuous performance surfaces. Second, a customizable weighted total scoring function was introduced to map multi-objective optimization onto a visualized, single-objective comprehensive scoring field. This not only enabled the precise identification of compliant variable intervals and the global optimum—converting discrete data into a continuous parameter space—but also provided structured training datasets for future machine learning models. Guided by this strategy and leveraging the core AI model of Surrogate-Based Optimization (SBO), the optimal 48.3D/63.9R formulation was rapidly identified with only a limited number of trials. Driven by a synergistic dual-mode mechanism—gas-phase radical quenching by 9,10-dihydro-9-oxa-10-phosphaphenanthrene-10-oxide (DOPO) and condensed-phase ceramic glaze formation by molten R-powder—this system achieved superior processability and mechanical integrity while meeting the impregnation and curing demands of large-tow carbon fiber composites. Beyond demonstrating exceptional gas-phase/condensed-phase synergistic flame retardancy, this work validates the proposed parameterized

optimization path as a critical bridge connecting small-sample experiments with future large-scale AI optimization. It offers a novel methodological paradigm for accelerating the intelligent design of high-performance flame-retardant resins tailored for large-tow composite materials, effectively overcoming current limitations in data scarcity and model adaptability.

Keywords: AI optimization strategy design; small sample optimization strategy; epoxy resin; DOPO; flame-retardant resin

1. Introduction

Carbon fiber composites offer advantages such as high specific strength, high specific modulus, and excellent design flexibility, and have already been applied in components including vehicle bodies, front hoods, bogies, and equipment compartments. Currently, the reinforcements used in these carbon fiber composites are exclusively small-tow carbon fibers, which suffer from high costs and low molding efficiency. With the increasing maturity of engineering-scale production technologies for large-tow carbon fibers, these materials can effectively address the issues of high composite part costs and low processing efficiency associated with small-tow carbon fibers.

The resin systems predominantly employed are based on bisphenol-A epoxy resins. Owing to their excellent mechanical performance, strong adhesion, and favorable electrical insulation, epoxy resins (EP) have found extensive applications in fields such as aerospace, electronics, and energy storage systems [1]. However, their aromatic backbone renders them inherently flammable, and the commonly used ambient-curing agents are aliphatic hardeners, which are also flammable. During combustion, these materials typically release substantial heat, produce dense smoke, and exhibit melt dripping—posing significant fire hazards in confined or high-value applications [2]. Driven by increasingly stringent environmental regulations, halogen-free flame-retardants have attracted growing research interest as viable alternatives to address this problem. In this context, 9,10-dihydro-9-oxa-10-phosphaphenanthrene-10-oxide (DOPO) has been widely recognized as a representative organophosphorus compound, primarily owing to its high phosphorus content and its efficient ability to trap radicals in the gas phase [3–7].

Extensive efforts have been devoted to enhancing DOPO's efficiency through molecular design or hybridization. For instance, P/N/S-containing derivatives [8,9], bi-hydroxyl-functionalized DOPO analogs [4], and tryptamine-based variants [10] have demonstrated improved flame retardancy at reduced loadings. Moreover, synergistic combinations of DOPO with inorganic fillers—such as nano-SiO_2 [11,12], wollastonite [13], or clay [14]—have been explored to simultaneously boost condensed-phase char formation and gas-phase inhibition. Notably, Liu *et al.* reported that low-melting organic-inorganic glasses can promote continuous char layers in epoxy/clay systems, significantly suppressing heat release [14]. Similarly, silicon-containing additives have shown multiple synergistic effects with DOPO derivatives, enhancing both flame retardancy and thermal stability [15].

Despite these advances, a persistent challenge remains: achieving UL-94 V-0 rating typically requires a high loading of DOPO, which inevitably plasticizes the matrix, lowers the glass transition temperature (Tg), and compromises mechanical integrity [5,10]. Although reactive DOPO derivatives can mitigate issues related to migration [4,16,17], they often involve complex synthesis routes and offer limited processability. An alternative strategy involves combining a moderate DOPO content with a tailored ceramic-forming agent that actively constructs a protective barrier during combustion, thereby further enhancing flame retardancy. Inspired by the glass-forming behavior observed in borophosphate systems [14], we propose a hybrid additive—termed R-powder—comprising Y_2O_3-stabilized borophosphate glass, fumed SiO_2, and zinc borate. This design leverages the melt-flow capability of low-melting-point glass to form a dense, highly stable vitreous layer, while DOPO provides complementary gas-phase radical quenching. However, the incorporation of flame-retardants inevitably degrades mechanical performance. Therefore, a multi-objective optimization balancing both mechanical properties and flame retardancy is essential for tailoring the composition of the flame-retardant system.

Currently, using machine learning for data optimization often requires a large amount of data, whereas materials experts can infer approximate optimization ranges with just a small amount of data. This is because there is a lack of an associative step before machine learning, meaning machines only receive a limited dataset. By plotting the data into composition-performance contour distribution maps and then having the machine read the data from these maps in a matrix format, it compensates for the missing link in the machine learning optimization process and significantly improves the computational efficiency of machine learning.

In recent years, machine learning (ML) has demonstrated tremendous potential in materials science, particularly in the design of polymeric materials where it has been employed for predicting polymer properties and optimizing formulation compositions [18]. Although ML has been applied to predict flame-retardancy and model mechanical properties of epoxy resin systems, most existing studies rely on large-scale experimental datasets, the acquisition of which is often costly and time-consuming. Furthermore, conventional ML methods struggle to generalize effectively under small-sample conditions and typically lack interpretability, often functioning as “black boxes.” To bridge this gap, this study proposes a dual-driven “parameterization-visualization” strategy. By transforming sparse experimental data into continuous performance surfaces, this approach provides high-quality input data for ML, thereby enabling effective optimization even in small-sample scenarios.

Compared to High-Throughput Experimentation (HTE), which exhaustively explores parameter spaces through extensive parallel experiments, our parameterization-visualization dual-driven strategy achieves superior data efficiency. By transforming sparse experimental data (only 7 data points) into continuous performance response surfaces, it locates global optima at minimal experimental cost—particularly advantageous for resource-intensive systems like flame-retardant resins, where it circumvents HTE’s inherent resource inefficiency. In contrast to conventional small-sample machine learning model, often treated as “black-box” systems lacking physicochemical interpretability, our strategy enhances optimization transparency through contour-plot visualization of composition-performance relationships, establishing a “white-box” optimization framework. This human-AI collaborative paradigm leverages computational power while integrating domain expertise, thereby elevating result credibility and interpretability without compromising optimization efficiency.

This paper systematically investigates the flame retardancy, mechanical properties, and thermal degradation behavior of DOPO/R-powder/Diglycidyl ether of bisphenol-A (DGEBA) epoxy composites. Building on an understanding of the flame-retardant mechanisms, a data association and machine vision approach is employed to optimize the flame-retardant resin system for large-tow carbon fiber composites using only a limited set of experimental data. This work provides a foundational basis for the future design and development of large-tow carbon fiber composites with both high safety and superior performance.

2. Methods

2.1. Materials

DGEBA, E-51 epoxy resin was provided by Sinopec Co., Ltd. (China). DOPO, 98% was purchased from Alfa Aesar (USA). 10-(2,5-dihydroxyphenyl)-10H-9-oxa-10-phospha-phenanthrene-10-oxide (DOPO-HQ) was supplied by Hubei Longxin Chemical Industry Co., Ltd. (China). Analytical-grade boric acid (H_3BO_3), yttrium oxide (Y_2O_3, 99.9%), calcium carbonate ($CaCO_3$, 99%), aluminum metaphosphate ($Al(PO_3)_3$, 98%), fumed silica (SiO_2), and zinc borate ($2ZnO·3B_2O_3·3.5H_2O$, Firebrake ZB) were obtained from Aladdin Reagent Co. (China). The curing agent 4,4′-diaminodiphenyl methane (DDM, 99%) was supplied by TCI (Japan). All chemicals were used as received without further purification.

2.2. Preparation of epoxy thermosets

Low-melting-point glasses with the nominal composition corresponding to RELTGF (Table 1) were synthesized via conventional melt-quenching. Stoichiometric amounts of B_2O_3, Y_2O_3, $CaCO_3$, and $Al(PO_3)_3$ were thoroughly ground and mixed in an agate mortar for 1 hour. Subsequently, this base glass powder was physically blended with fumed SiO_2 and zinc borate at a mass ratio of 14:10:4 using an Al_2O_3 mixer for 30 minutes to obtain the final hybrid additive, denoted as R-powder.

Table 1. Composition design of RELTGF (wt.%).

ID	B_2O_3	Y_2O_3	CaO	$Al(PO_3)_3$
RELTGF	45	15	30	10

Seven epoxy formulations were prepared: neat EP, 30D, 60D, 90D, 30D/60R, 60D/60R and 90D/40R (where "R" denotes R-powder). The detailed compositions are listed in Table 2. For composite samples, DOPO was first dissolved in DGEBA resin at 160 °C with vigorous stirring for 40 min to ensure complete dissolution. R-powder was then added, and the mixture was stirred at 80 °C for 60 min. The stoichiometric amount of DDM curing agent was introduced at room temperature, and the mixture was degassed under vacuum before being poured into molds. Curing was carried out at 90 °C for 2 h.

Table 2. Formulations of epoxy thermosets (phr).

ID	DGEBA	DDM	DOPO-HQ	R-powder
EP	100	30	0	0
30D	100	30	30	0
60D	100	30	60	0
90D	100	30	90	0
30D/60R	100	30	30	60
60D/60R	100	30	60	60
90D/40R	100	30	90	40

2.3. Characterization

The chemical structure and interactions in the cured epoxy systems were examined by Fourier-transform infrared spectroscopy (FTIR) using a Thermo Nicolet Nexus 670 spectrometer over the range of 4000–400 cm^{-1} with KBr pellets. Tensile properties were determined on a Kexin WDW-100 universal testing machine, with a crosshead speed of 2 mm/min; at least 3 specimens (2 mm × 13 mm × 125 mm) were tested for each formulation. Due to sample geometry constraints, non-standard specimen dimensions were employed. The testing procedure strictly complied with the environmental conditions, loading rate, and data processing requirements specified in GB/T 2567-2021. All the collected data is only applied to compare the relative performance among specimens from the identical batch, and it cannot correspond to the absolute property values tested by standard-sized samples. Vertical burning tests (UL-94, GB/T 2408-2008) and limiting oxygen index tests (LOI, GB/T 2406.2-2009) with oxygen-nitrogen mixed gas were adopted to assess the flame-retardant performance of the materials. Field-emission scanning electron microscopy (SEM, Quanta 250 FEG) at an operating voltage of 5 kV was utilized to observe the morphological structure of char residues generated from cone calorimetry tests or UL-94 tests. All test samples were sprayed and plated with a thin gold film before microscopic imaging.

2.4. Calculation method and details

In this study, OriginPro software was utilized to generate contour plots depicting the relationship between DOPO-HQ/R powder composition and two key performance metrics: tensile strength and limiting oxygen index (LOI), based on a limited set of experimental data. The LOI is defined as the minimum concentration of oxygen in a nitrogen-oxygen mixture required to sustain flaming combustion, expressed as a volume percentage, and serves as a critical indicator for evaluating the flame retardancy of materials. To quantitatively extract information from these contour maps, a uniform 21 × 21 grid was superimposed over each plot, and corresponding Z-values at each grid node were digitized. The extracted data were subsequently normalized using a defined scoring scheme. Under predefined constraints on material performance criteria, the feasible compositional ranges satisfying the target specifications were identified, enabling the determination of the optimal formulation and its underlying compositional–property trends.

3. Results

3.1. Synthesis and characterization

The successful synthesis of the amorphous low-temperature glass and the integrity of the R-powder hybrid were first confirmed by FTIR analyses. As shown in Figure 1a, combined with the data shown in Figure 1a, as the DOPO-HQ loading increases (30, 60, and 90 parts), the characteristic absorption peaks of the epoxy resin—located at 824, 1232, and 2921 cm^{-1}—show no significant shift in position, nor are any new peaks observed. This indicates that DOPO-HQ is primarily incorporated into the system via physical blending rather than forming covalent bonds or altering the main-chain structure of the epoxy matrix. However, when the DOPO-HQ content reaches 60 parts, as illustrated in Figure 1a, the intensities of the peaks at 824 and 1232 cm^{-1} noticeably decrease. Furthermore, the absorption peak at approximately 2435 cm^{-1}, assigned to the stretching vibration of P–H bonds, completely disappeared in the DOPO-modified samples. Concurrently, a stretching vibration peak of P=O emerged at 1232 cm^{-1}, and characteristic absorption of P–O–Ph was detected in the range of 750–755 cm^{-1}.This reduction is likely attributed to a dilution effect and intermolecular interactions—such as hydrogen bonding or dipole–dipole interactions—between the phosphorus-containing groups (e.g., P=O) in DOPO-HQ and ether linkages or hydroxyl groups in the epoxy resin, which affect the vibrational dipole moments of these functional groups. In contrast, as shown in Figure 1b, the addition of R powder (ceramic filler) causes no discernible changes in either peak positions or intensities, further confirming that this inorganic filler remains chemically inert within the tested range and is merely dispersed physically in the matrix. Overall, the flame-retardant action of DOPO-HQ appears to operate predominantly through physical barrier effects and gas-phase/condensed-phase mechanisms, rather than through chemical modification of the epoxy network.

(a)

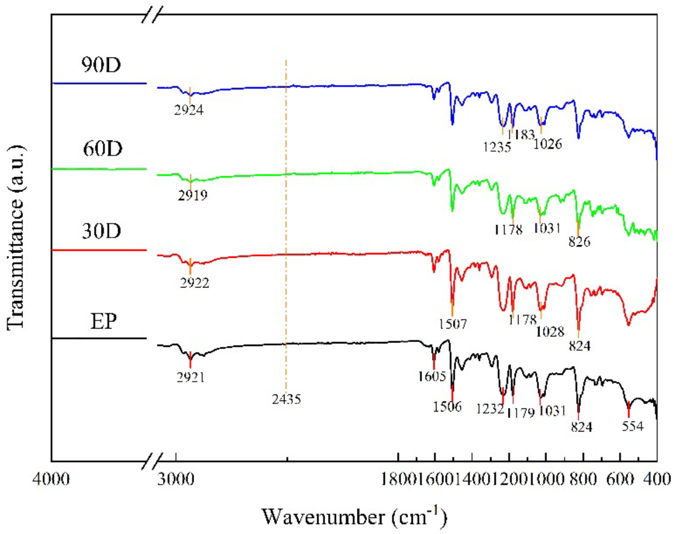

(b)

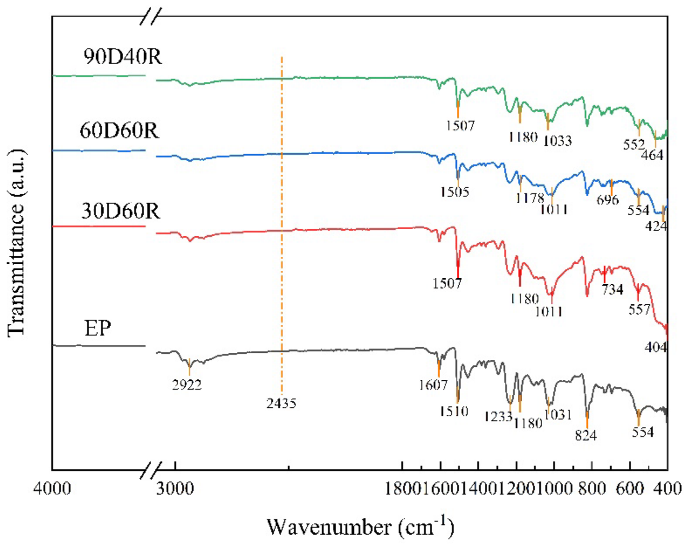

Figure 1. FTIR spectra of **(a)** epoxy resin with different DOPO-HQ content, and **(b)** epoxy resin with different DOPO-HQ content added with R powder.

3.2. Mechanical property

The tensile strength of epoxy composites is highly sensitive to the nature and content of additives, as they can either reinforce the matrix or act as stress concentrators. As shown in Figure 2, neat epoxy (Neat EP) exhibits a tensile strength of 54.8 MPa. Adding only DOPO into the system can bring obvious mechanical property loss. For mechanical strength values, the 30D sample falls to 19.5 MPa, 60D and 90D samples show even lower values at 18.8 MPa and 17.8 MPa in sequence. Such mechanical performance degradation occurs due to the plasticization brought by DOPO. The flexible heterocyclic structure of DOPO breaks the regular arrangement of molecular chains and lowers the overall crosslink density of the composite material. More critically, at higher loadings, DOPO approaches its solubility limit within the epoxy network, inducing micro-scale phase separation that further compromises load transfer efficiency. In stark contrast, composites containing R-powder demonstrate a significant advantage in mechanical retention. Despite a high total solid loading of 60 phr, the 30D/60R formulation achieves a tensile strength of 22.8 MPa. Compared to the 30D sample, which has a lower total additive content, this unexpected enhancement is attributed to the well-dispersed R-powder particles—particularly the nano-sized fumed SiO_2 and amorphous glass phase—which provide effective reinforcement, restrict polymer chain mobility, and improve DOPO dispersion. However, this dispersing effect gradually diminishes as the DOPO content increases. By the 90D/40R stage, the mechanical properties of the material deteriorate further.

To identify the optimization interval, contour plots illustrating the relationship between DOPO-HQ, R-powder, and tensile properties were constructed (as shown in Figure 3). By extracting data from these contours, a data matrix linking DOPO-HQ and R-powder contents to tensile performance was established, laying the groundwork for subsequent multi-objective comprehensive performance optimization.

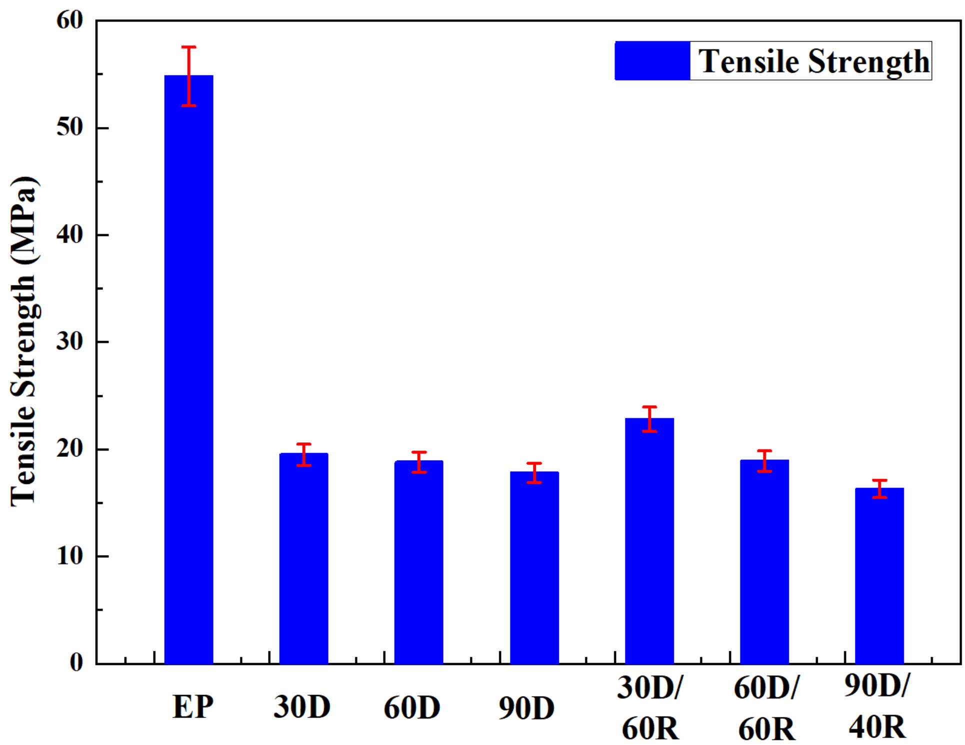

Figure 2. Tensile strength of neat EP and flame-retardant composites. Error bars represent standard deviation from 3 replicates.

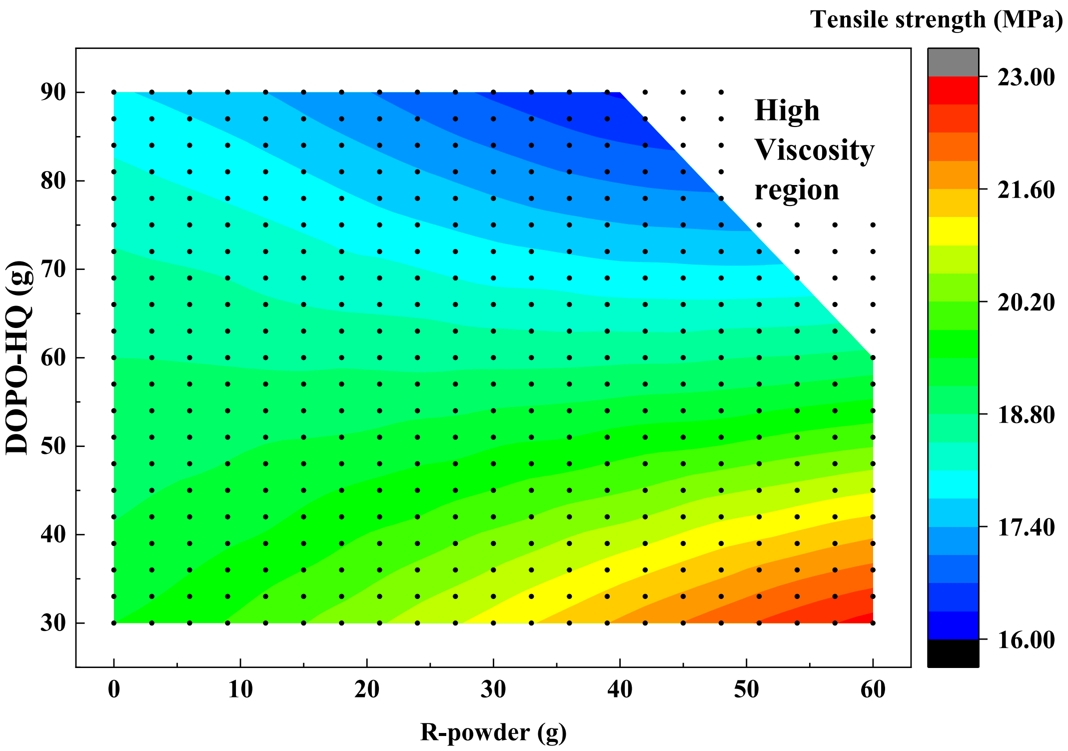

Figure 3. Contour plots and matrix data extraction for DOPO-HQ, R-powder, and tensile properties.

3.3. Flame-retardant performance

The high flammability of the Neat EP is clearly confirmed by the experimental data. As illustrated in Figures 4 and 5, the sample burns vigorously and produces severe flaming drips. More critically, it fails to self-extinguish within the required 30 s, resulting in a UL-94 No Rating. The LOI value is also quite low, recorded at only 18%. To capture these behaviors comprehensively, we employed both vertical burning (UL-94) and LOI tests. Using these two methods together is necessary because they complement each other; they allow us to evaluate not just the ignition resistance, but also the self-extinguishing ability and combustion sustainability of the composites. As shown in Figures 4 and 5, Neat EP burns vigorously with severe flaming drips, fails to self-extinguish within 30 s (rated UL-94 No Rating), and exhibits a low LOI of 18%, confirming its high flammability. The incorporation of DOPO alone improves performance in a dosage-dependent manner: the 30D sample achieves a UL-94 V-2 rating (total afterflame time of 59 s, but with flaming drips that ignite cotton) and an LOI of 22%. Increasing the DOPO content to 60 phr (60D sample) eliminates dripping, yielding a V-0 rating (afterflame time < 30 s, no cotton ignition) and raising the LOI to 25%. Consequently, further enhancement of the limiting oxygen index is necessary.

Observations from Figure 4 and Figure 5 indicate that R-powder addition enhances flame retardancy to a certain extent. The effect works through synergistic condensed-phase action. The 30D/60R composite achieves a UL-94 V-0 rating. It has average afterflame times of only 3 s for the first ignition, and 4 s for the second. Its LOI is 24%. The LOI value is relatively low. Still, the material delivers excellent self-extinguishing properties under ambient air conditions.

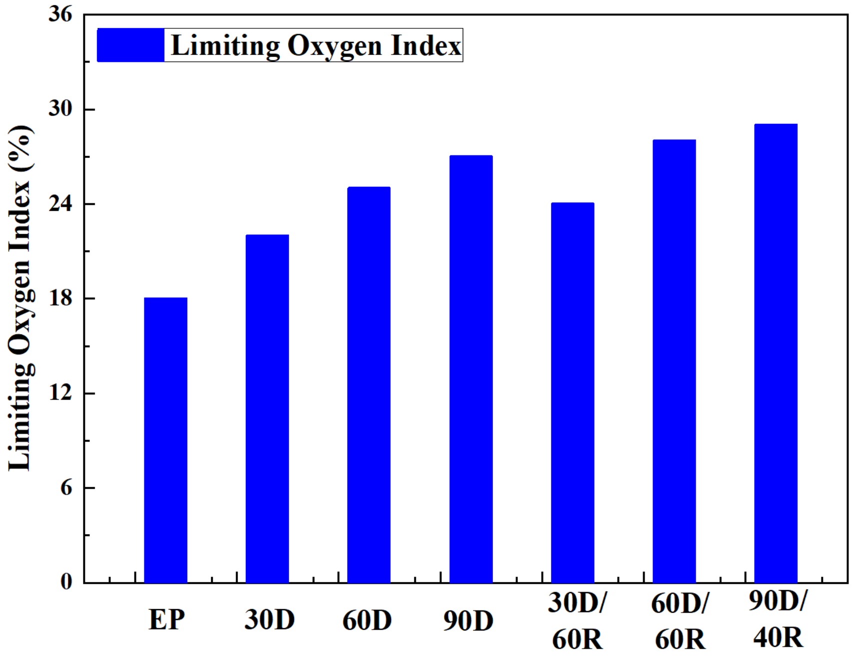

Figure 4. UL-94 ratings and LOI values of epoxy composites.

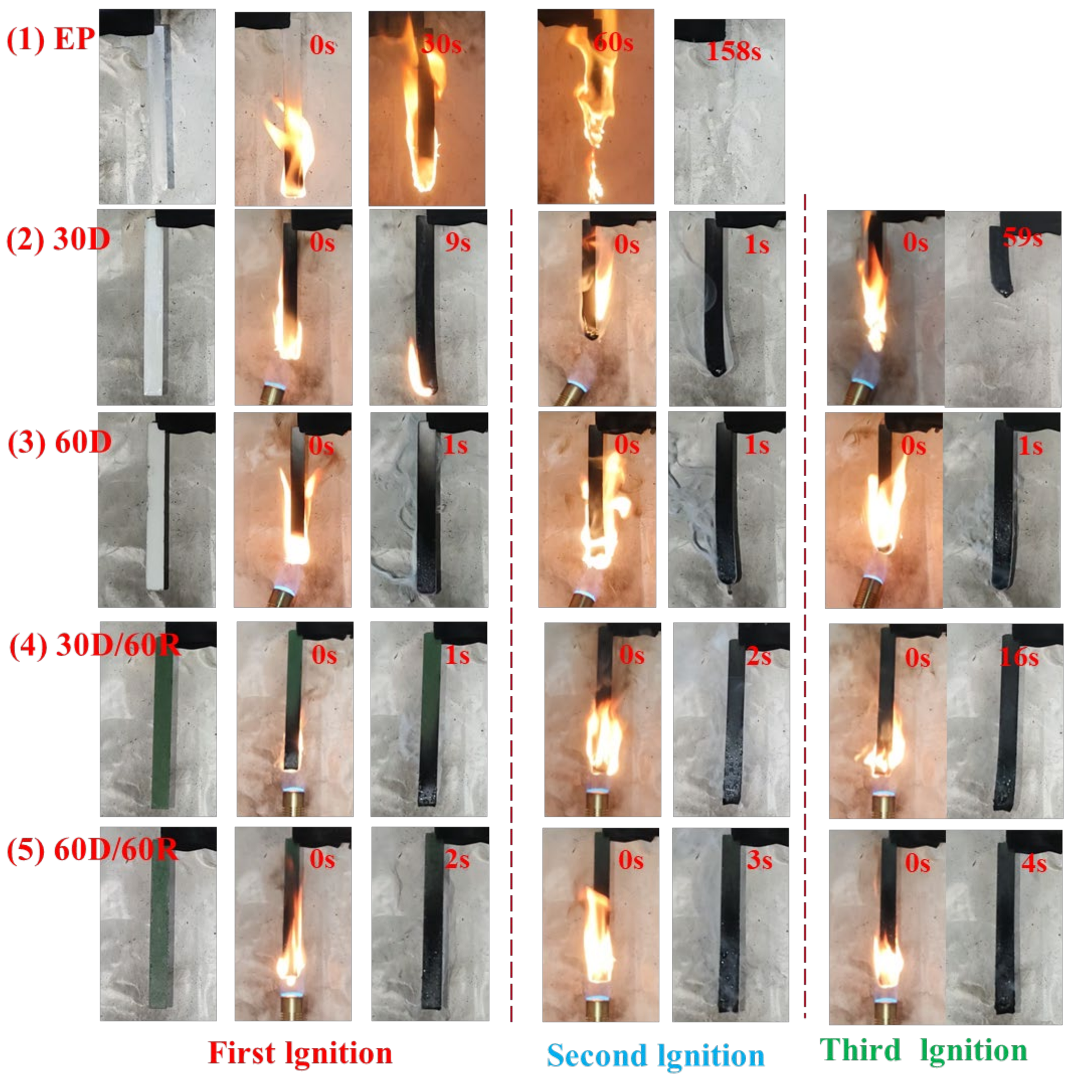

Figure 5. Digital photographs of specimens during UL-94 testing.

Similarly, the 60D/60R formulation also achieved a V-0 rating (LOI = 28%), confirming the robustness of the R-powder's effect. This significant improvement stems from a dual-mode mechanism: DOPO releases ·PO and ·HPO radicals in the gas phase to scavenge ·H and ·OH radicals, while R-powder melts and flows during combustion (onset at ~520 °C) to form a continuous, glassy glaze layer on the surface. This protective layer works as physical barrier. It inhibits heat feedback, obstructs oxygen diffusion and captures volatile decomposition products. This process isolates flame fuel sources and stops the material from re-igniting. None of the samples filled with R-powder produced flaming drips during combustion. The dense and viscous glaze layer restricts the flow of molten polymer effectively.

These results demonstrate that R-powder enables a paradigm shift: instead of relying solely on high organophosphorus loadings, a moderate amount of DOPO can be leveraged in concert with a tailored ceramic-forming additive to achieve superior fire safety. The 60D/60R system, in particular, represents an optimal balance—delivering V-0 rating and high LOI while mitigating the mechanical and processing drawbacks associated with excessive DOPO.

To identify the optimization interval, contour plots illustrating the relationship between DOPO-HQ, R-powder, and the LOI were constructed (as shown in Figure 6). By extracting data from these contours, a data matrix linking DOPO-HQ and R-powder contents to LOI was established, laying the groundwork for subsequent multi-objective comprehensive performance optimization.

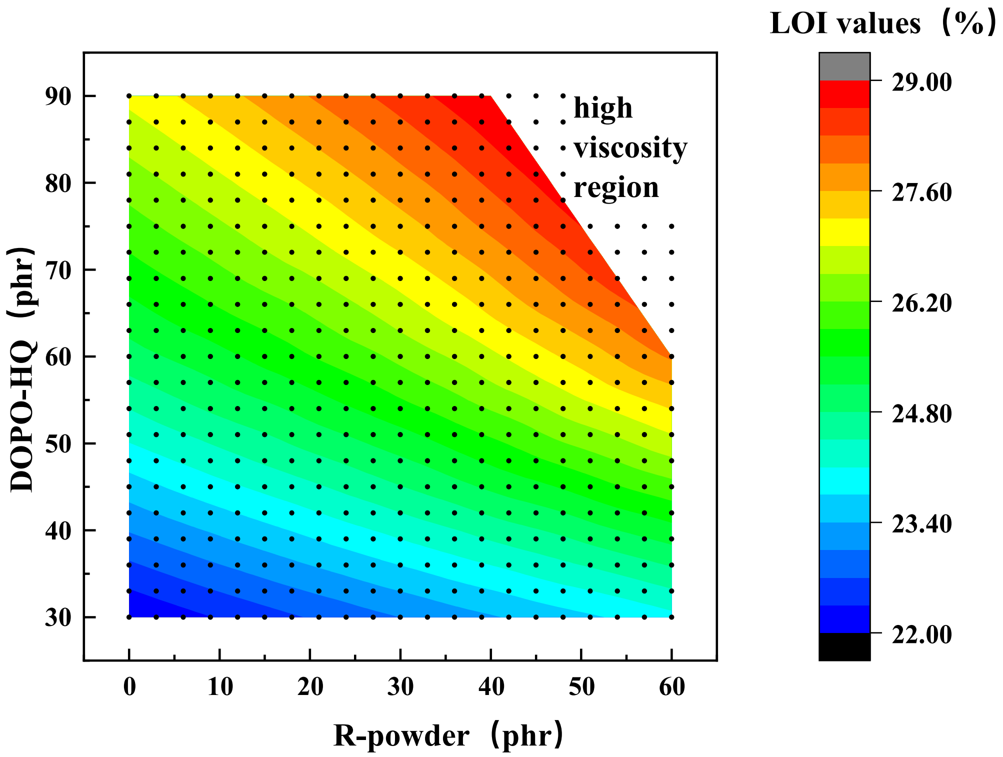

Figure 6. Contour plots and matrix data extraction for DOPO-HQ, R-powder, and LOI.

As shown in Figure 7, Thermogravimetric analysis (TGA) revealed that neat EP exhibited an initial decomposition temperature at 5% mass loss ($T_{5\%}$) of 162 °C, a peak temperature of maximum mass loss rate (T_{max}) at 320 °C, a maximum mass loss rate (MLR) of 2.8 %/°C, and zero char residue at 800 °C (R_{800}). Upon incorporation of DOPO-HQ or DOPO-HQ/glass powder hybrid systems, all modified samples showed increased $T_{5\%}$ and R_{800} values alongside reduced MLR. For DOPO-HQ alone, sample 30D displayed a reduced $T_{5\%}$ of 147 °C (9.3% lower than EP), attributed to low-temperature cleavage of P–O bonds releasing free radicals. With increasing DOPO-HQ content, $T_{5\%}$ gradually recovered, MLR consistently decreased, and R_{800} rose to 7.51%, owing to the formation of a phosphorus-containing char layer. Hybrid systems with glass powder further enhanced thermal stability: 30D/60R achieved a $T_{5\%}$ of 251 °C, an MLR of 0.83 %/°C, and an R_{800} of 24.97%, while 60D/60R exhibited an even lower MLR of 0.49 %/°C and an R_{800} of 25.93%. The synergistic ceramification between high-temperature-molten glass powder and the phosphorus-containing char layer suppressed pyrolytic volatiles, elevating the char residue by two orders of magnitude compared to DOPO-HQ-only systems. The hybrid systems significantly improved thermal stability through combined gas-phase radical scavenging by DOPO-HQ and condensed-phase ceramic barrier formation by glass powder, maintaining stability below 250 °C to meet prepreg processing requirements.

(a) (b)

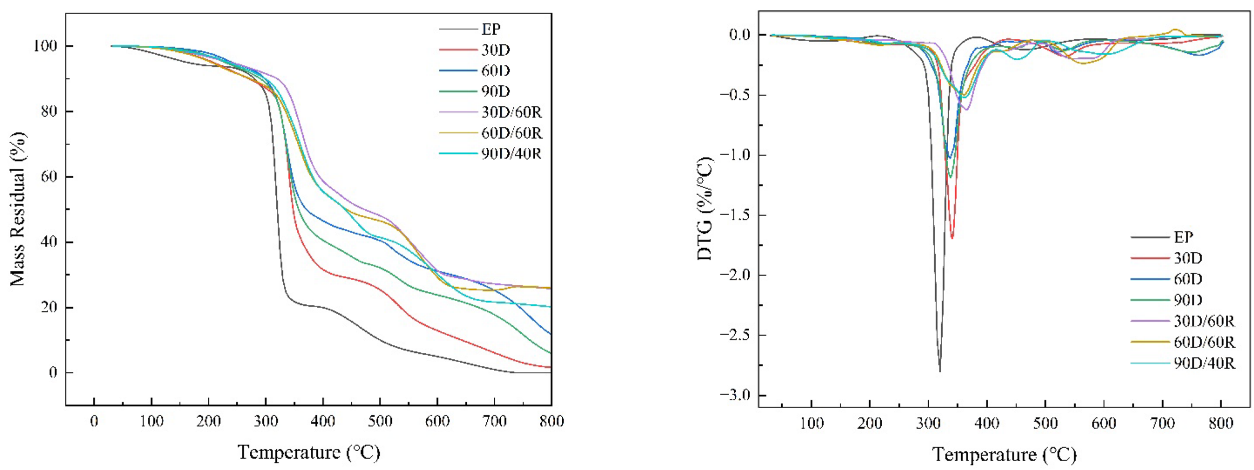

Figure 7. Comparative TGA and derivative thermogravimetry (DTG) curves of DOPO-HQ and R powder.

3.4. Morphology characterization

The microstructure of the char residues after UL-94 vertical burning tests provides direct visual evidence of the flame-retardant mechanism and was characterized by field-emission scanning electron microscopy (FE-SEM). As shown in Figure 8a, the residue of Neat EP is virtually absent; the surface has been burned into a uniform, flammable carbon layer that offers no barrier against oxidation. The 30D sample (Figure 8b) exhibits localized combustion irregularities due to DOPO's interference with the combustion chain segments, resulting in the formation of circular voids on the surface carbon layer. Concurrently, the uniform distribution of phosphorus (P) indicates that increasing DOPO content contributes to flame retardancy, yet remains insufficient. This explains why the sample, despite its high DOPO loading, failed to achieve a V-0 rating.

Composites with R-powder show a completely different charring behavior. They form coherent, continuous surface layers. These layers fully encapsulate the underlying base material. The char layer of the 30D/60R sample (Figure 8c) has a higher oxide content. It sticks tightly to the unburned epoxy substrate. This layer works as an effective barrier to block heat and mass transfer. The intact structure of this char layer is the direct reason for the fast self-extinguishing effect. It also explains why no dripping occurs during UL-94 tests.

In parallel, in the gas phase, DOPO decomposes at lower temperatures (300–400 °C), releasing phosphorus-containing radicals in the gas phase, these morphological observations validate the proposed dual-mode flame-retardant mechanism: while DOPO acts in the gas phase, R-powder facilitates the formation of an oxide-based ceramic in the condensed phase, enabling the 30D/60R sample to achieve effective flame retardancy under ambient air conditions.

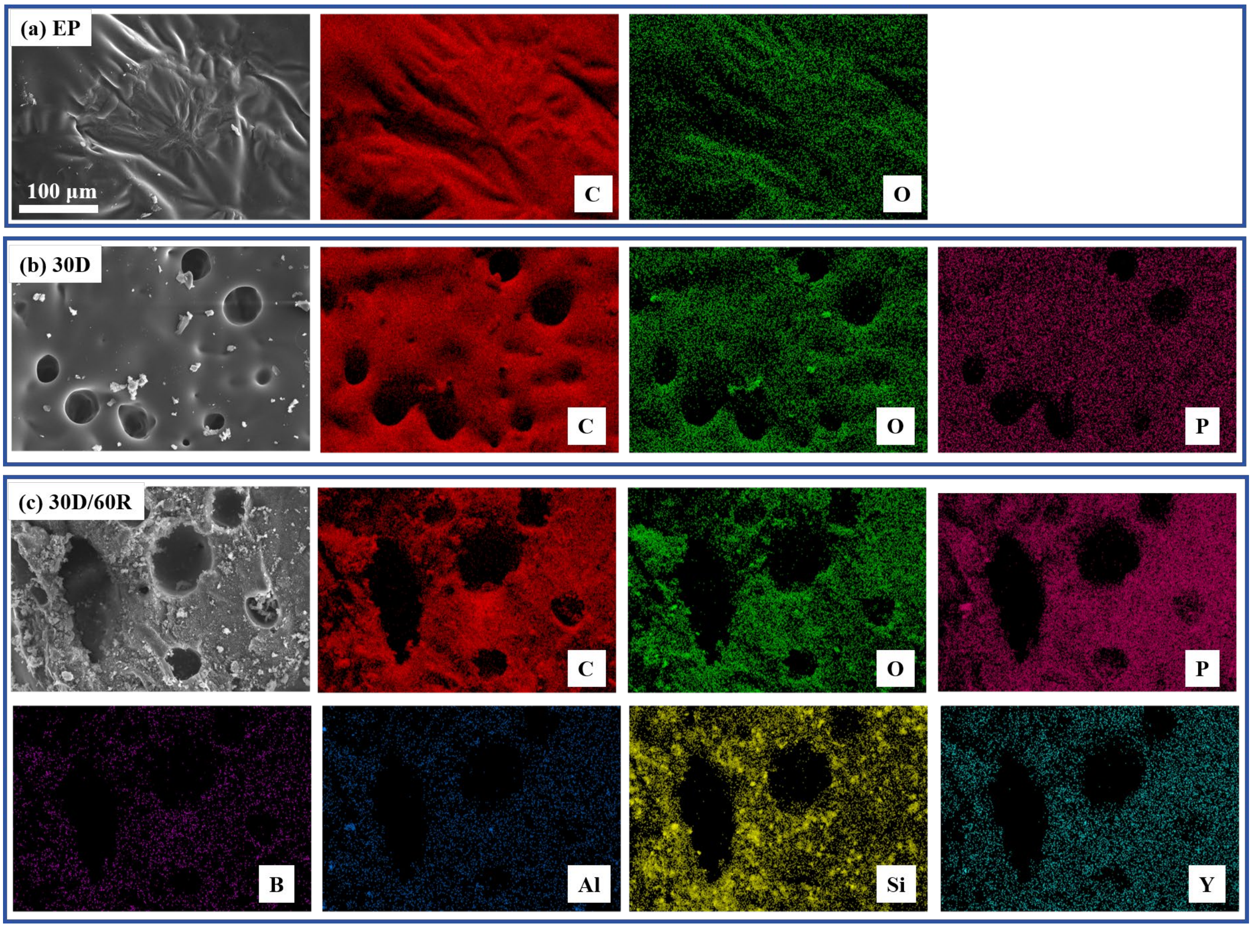

Figure 8. SEM images of char residues after UL-94 testing: **(a)** EP, **(b)** 30D, **(c)** 30D/60R.

The dense ceramic glaze layer in the char residue of sample 30D/60R originates from the synergistic interaction of B, Al, Si, and Y elements at elevated temperatures. R powder contains zinc borate and borophosphate glass, which begin to melt at the early combustion stage. The released B_2O_3 lowers the overall melting point of the composite system and facilitates the formation of liquid-phase substances. Gaseous SiO_2 meanwhile reacts in situ with aluminum metaphosphate [$Al(PO_3)_3$] and Y_2O_3, producing yttrium phosphate (YPO_4) and aluminosilicate ceramic substances with high melting points. Yttrium element serves as a network intermediate, it can improve the mechanical strength of the formed glaze layer. Driven by surface tension, the molten phase rich in B, Si, Al and Y spreads over the char layer surface and fills microscale voids and cracks. After cooling treatment, this molten substance turns into an integrated and intact glass-ceramic composite glaze layer. The formed dense layer provides strong physical barrier protection, it restricts heat transfer, oxygen penetration and the escape of combustible volatile products. Combined with the gas-phase radical scavenging effect of DOPO, such condensed-phase protection achieves well-coordinated spatial and temporal effects, constructing a complete gas-condensed dual-phase synergistic flame-retardant mechanism.

3.5. Data-efficient design

By adopting OriginPro software as the machine vision data extraction tool, contour plot image data from DOPO-HQ-R powder-tensile properties and DOPO-HQ-R powder-LOI contour diagrams were extracted using a 21 × 21 matrix for machine vision reading. The obtained data were processed according to normalized scoring rules, as defined in Equation (1). Under the constraints of specified material performance indicators, composition intervals meeting the required performance criteria were determined, along with the optimal composition and its variation pattern. Here, the tensile performance indicator was set at 18 MPa with a scoring weight of 2, while the LOI performance indicator was 26% with an identical scoring weight of 2.

$$[OS = \left(\frac{c_1 \times S}{S_1} + \frac{c_2 \times LOI}{LOI_1}\right) \cdot f_1 \cdot f_2] \quad (1)$$

$$[f_1 = \mathrm{f(x)} = \begin{cases} 0, & \mathrm{s} < s_1 \\ 1, & \mathrm{s} \geq s_1 \end{cases}] \quad (2)$$

$$[f_2 = \mathrm{f(x)} = \begin{cases} 0, & LOI < LOI_1 \\ 1, & LOI \geq LOI_1 \end{cases}] \quad (3)$$

OS represents the material overall score, c_1 and c_2 are scoring weights, s denotes tensile properties, LOI refers to limiting oxygen index, s_1 is the tensile property indicator, s_2 is the LOI property indicator, while f_1 and f_2 are qualified parameters.

The optimal composition with the best overall performance can be intuitively identified from the composition-score contour map. The obtained map is presented in Figure 9, it directly shows the composition intervals that meet the required performance indicators and the score variation trends. The final recommended composition is adjusted from the original formulation, with an R powder loading of 60 phr and a DOPO-HQ loading of 45 phr. This composition gives a predicted tensile strength of 20.5 MPa and a predicted LOI value of 26.2%.

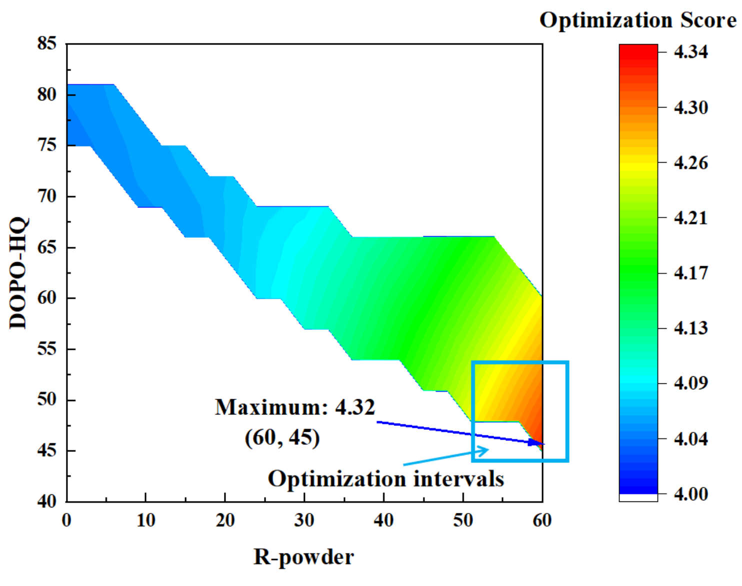

Figure 9. Data-efficient design composition-score contour map.

3.6. Machine learning optimization

It can be observed that, based on efficient design strategies, researchers can rapidly optimize and obtain optimal results. Similar optimization strategies make it possible for AI to rapidly locate the best data points. This work therefore adopts such a method and applies machine-learning-based Surrogate-Based Optimization (SBO) for further data refinement. Gaussian Process Regression (GPR) serves as the core AI algorithm of SBO, this probabilistic regression method fits experimental cases with limited sample size and high testing cost. Unlike traditional neural networks that rely on massive datasets to train weights, GPR defines spatial correlations between data points via kernel functions (e.g., Radial Basis Function (RBF)) to fit discrete experimental observations into a continuous, smooth response surface. Its distinct advantage lies in its ability to not only predict the mean of the target value but also simultaneously quantify prediction uncertainty (variance), thereby providing confidence assessments in data-sparse regions. Within the optimization workflow, this model acts as a "virtual experimenter," constructing a computationally inexpensive mathematical surrogate function to replace costly real-world experiments. This enables global optimization algorithms (such as Differential Evolution) to search millions of virtual points in milliseconds, efficiently balancing the strategy of "exploiting known high-score regions" with "exploring unknown high-uncertainty areas," ultimately pinpointing the global optimum with minimal experimental trials, making it particularly suitable for parameter optimization of black-box functions in fields like materials science and chemical formulation.

The optimization yielded the following results: R-powder: 48.3 phr, DOPO-HQ: 63.9 phr, with a predicted maximum Score of 4.81 and a predicted uncertainty (Std) of 0.61. Notably, the AI identified a theoretical peak higher than any value in the existing dataset. These findings demonstrate that, even with the limited data from the original experiments, AI achieved performance comparable to expert predictions while successfully inferring superior optimal values. This confirms that the proposed design optimization strategy is highly effective when applied to AI-driven analysis. The execution code is available in the Data and code availability section.

3.7. Experimental validation and performance evaluation

To validate the reliability of the surrogate model-based optimization results, experimental verification was conducted using the optimal parameters predicted by the model. Composite specimens were prepared using the predicted optimal formulation (48.3 parts R powder and 63.9 parts DOPO-HQ), and their flame retardancy and mechanical properties were evaluated according to relevant standards.

The experimental results are presented in Table 3. The experimental results demonstrate that the composite prepared with the optimized formulation achieved a UL-94 V-0 rating. In the vertical burning test, the average afterflame times following the first and second ignitions were 2 s and 3 s, respectively, with no ignition of the surgical cotton and no dripping observed during combustion. Testing results show that the composite obtains a LOI value of 25.9%. This experimental result has a 1.15% relative error, when compared with the model prediction of 26.2%. For mechanical performance, the tested tensile strength reaches 21.3 MPa. It presents a relative error of 3.9% relative to the predicted tensile strength of 20.5 MPa.

Experimental data and model predictions show great consistency. All deviation values stay within acceptable error ranges. It proves that the proposed optimization strategy is reliable and accurate. This method can effectively predict material performances and guide the design of composite formulations.

Table 3. Experimental validation of the surrogate model predictions for the optimal formulation.

ID	Tensile strength (MPa)	UL-94	LOI (%)
63.9D/48.3R	21.3	V-0	26.2

4. Conclusion

(1) In response to the critical need for flame-retardant resins tailored to carbon fiber composites, this study successfully developed a high-performance epoxy system by integrating a novel ceramic-forming hybrid additive (R-powder) with moderate loadings of DOPO. To overcome the inherent challenges of machine learning in small-sample optimization, we pioneered a "parameterization-visualization" dual-driven strategy. This approach transforms sparse bivariate experimental data into a continuous, high-resolution performance matrix via contour interpolation and employs a customizable weighted scoring function to map multi-objective goals onto a single visualized field. This strategy not only bypasses the data sparsity bottleneck but also establishes a standardized, AI-accessible pathway for future material design. Guided by this framework and leveraging the core AI model of SBO, we rapidly identified the optimal 48.3D/63.9R formulation, achieving superior fire safety and mechanical integrity while ensuring the processability required for impregnation.

(2) The exceptional performance of the optimized system stems from a robust synergistic dual-mode flame-retardant mechanism. In the condensed phase, R-powder melts during combustion to form a continuous, crack-free, and thermally stable glassy glaze layer reinforced by YPO_4, $Zn_3(PO_4)_2$, and Ca–Si–B–P ceramic phases, effectively shielding the polymer matrix from heat, oxygen, and volatile fuel diffusion. Simultaneously, in the gas phase, DOPO decomposes to release ·PO/·HPO radicals that efficiently quench highly reactive ·H/·OH species, interrupting the combustion chain reaction. This complementary action allows for significant reduction in organophosphorus usage compared to conventional high-loading systems, thereby mitigating the migration issues, mechanical degradation, and processing difficulties often associated with excessive DOPO. Consequently, the study shifts the paradigm from simple additive-dominated formulations to function-integrated, multi-phase cooperative systems specifically engineered for demanding composite applications.

Data availability statement

The code is available at the link below: https://github.com/eeepoe2009/Intelligent-optimization-of-flame-retardant-material-performance/releases/tag/flame-retardant-material-v1.

Declaration of generative AI and AI-assisted technologies

During the preparation of this work, the authors used "Qwen" (developed by Alibaba Cloud) to assist with the translation of specific sentences and to polish the language for improved readability. After using this tool, the authors reviewed and edited the content as needed. The authors take full responsibility for the content of the manuscript.

Acknowledgments

This work was supported by the National Science and Technology Major Project of China (Grant No. 2024ZD0602200). The authors would also like to express their gratitude to CRRC Advanced Composites Co., Ltd. for its [technical support/provision of experimental mate- rials/financial support].

Authors' contribution

P.W.: writing—original draft, writing—review and editing, project administration, validation, data curation, formal analysis, investigation and methodology; Y.W.: writing—original draft, writing—review and editing and data curation; Z.W.: investigation; supervision; writing—review and editing; Y.Q.: investigation, methodology, supervision; L.Z.: investigation, supervision and validation; L.S.: funding acquisition, project administration and resources; J.H.: funding acquisition, project administration and resources; S.Y.: funding acquisition, project administration and resources; Z.Y.: funding acquisition, project administration and resources. All authors have read and agreed to the published version of the manuscript.

Conflicts of interest

Lei Shi, Jiajie He, Shujing Yue and Zhaoding Yao are employees of CRRC Advanoed Composites Co., Ltd. The authors declare that this affiliation does not influence the design, analysis, interpretation, or presentation of the results reported in this manuscript. The authors declare no other conflicts of interest.

References

[1] Luo Y, Hou Y, Zhang P, Xu P, Luo Z, *et al*. Dual-effect integration of thermal management and flame retardancy for 3D boron nitride/epoxy/benzoxazine composites. *Adv. Funct. Mater.* 2026, 36(32):e26998.

[2] Velencoso MM, Battig A, Markwart JC, Schartel B, Wurm FR, *et al*. Molecular firefighting—how modern phosphorus chemistry can help solve the challenge of flame retardancy. *Angew. Chem. Int. Ed.* 2018, 57(33):10450–10467.

[3] Schäfer A, Seibold S, Lohstroh W, Walter O, Döring M, Synthesis and properties of flame-retardant epoxy resins based on DOPO and one of its analog DPPO. *J. Appl. Polym. Sci.* 2007, 105(2):685–696.

[4] Zhang J, Duan H, Cao J, Zou J, Ma H, A high-efficiency DOPO-based reactive flame-retardant with bi-hydroxyl for low-flammability epoxy resin. *J. Appl. Polym. Sci.* 2021, 138(14):50165.

[5] Wei Z, Gu X, Wu J, Wei M, Yu Q, *et al.* Performance comparison of epoxy resins modified with diphenylphosphine oxide and DOPO. *Fire Mater.* 2019, 43(7):892–902.

[6] Zhang Y, Yu B, Wang B, Liew KM, Song L, *et al*. Highly effective P-P synergy of a novel DOPO-based flame retardant for epoxy resin. *Ind. Eng. Chem. Res.* 2017, 56(5):1245–1255.

[7] Yang B, Li X, Wang L, Zhang Y, Cui J, *et al.* An efficient flame retardant for epoxy resin: preparation and pyrolytic behaviour. *High Perform. Polym.* 2019, 31(9–10):1009–1019.

[8] Jian R, Wang P, Duan W, Wang J, Zheng X, *et al*. Synthesis of a novel P/N/S-containing flame-retardant and its application in epoxy resin: thermal property, flame retardance, and pyrolysis behavior. *Ind. Eng. Chem. Res.* 2016, 55(44):11520–11527.

[9] Wang P, Xia L, Jian R, Ai Y, Zheng X, *et al*. Flame-retarding epoxy resin with an efficient P/N/S-containing flame-retardant: preparation, thermal stability, and flame retardance. *Polym. Degrad. Stab.* 2018, 149:69–77.

[10] Chen R, Dai S, Guo T, Tang H, Fan Y, *et al*. Transparent low-flammability epoxy resins with improved mechanical properties using tryptamine-based DOPO derivative. *Polym. Eng. Sci.* 2019, 59(10):2008–2015.

[11] Häublein M, Peter K, Brückner A, Altstädt V. Evaluation of DOPO and nano-silica modified epoxy resin systems as low viscous, flame-retardant additives for infusion and injection processing of carbon fiber reinforced plastics. *Key Eng. Mater.* 2019, 809:3–8.

[12] Häublein M, Peter K, Bakis G, Mäkimieni R, Altstädt V, *et al*. Investigation on the flame-retardant properties and fracture toughness of DOPO and nano-SiO_2 modified epoxy novolac resin and evaluation of its combinational effects. *Materials* 2019, 12(9):1528.

[13] Wang Z, Gao X, Li W. Epoxy resin/cyanate ester composites containing DOPO and wollastonite with simultaneously improved flame retardancy and thermal resistance. *High Perform. Polym.* 2020, 32(6):710–718.

[14] Yu D, Kleemeier M, Wu G, Schartel B, Liu W, *et al*. A low melting organic-inorganic glass and its effect on flame retardancy of clay/epoxy composites. *Polymer* 2011, 52(10):2120–2131.

[15] Wang K, Huang W, Tian Q, Tu C, Yang C, *et al*. Multiple synergistic effects of silicon-containing flame-retardants and DOPO derivative enhance the flame retardancy of epoxy resin. *Polym.-Plast. Technol. Mater.* 2024, 63(10):1294–1305.

[16] Luo H, Rao W, Liu Y, Zhao P, Wang L, *et al*. Novel multi-element DOPO derivative toward low-flammability epoxy resin. *J. Appl. Polym. Sci.* 2020, 137(46):49427.

[17] Wang P, Cai Z. Highly efficient flame-retardant epoxy resin with a novel DOPO-based triazole compound: thermal stability, flame retardancy and mechanism. *Polym. Degrad. Stab.* 2017, 137:138–150.

[18] Baral A, Chowdhury MA, Hasan MJ, Nir AA, Arnab MB, *et al*. Prediction of mechanical properties of carbon fiber/epoxy composite modified by nanoparticles using multiple explainable machine learning algorithms. *Mater. Des.* 2025, 257:114537.